Journal of Coastal Research	00	00	000–000	Charlotte, North Carolina	Month 0000

Nearshore Morphological Changes due to Severe Cyclonic Storm Activity along the East Coast of India

J. Guru Prasath[†‡]*, S.A. Sannasiraj[†], and P. Chandramohan[‡]

[†]Ocean Engineering Department
Indian Institute of Technology, Madras
Chennai 600036, India

[‡]Indomer Coastal Hydraulics
Chennai 600087, India

www.cerf-jcr.org

www.JCRonline.org

ABSTRACT

Guru Prasath, J.; Sannasiraj, S.A., and Chandramohan, P., 000. Nearshore morphological changes due to severe cyclonic storm activity along the east coast of India. *Journal of Coastal Research,* 00(00), 000–000. Charlotte (North Carolina), ISSN 0749-0208.

Nearshore waves, wind, and tidal current mobilize seabed sediments; sort, transport, and redistribute the sediments; and modify the nearshore seabed morphology. Waves play a dominant role in morphological changes among winds, waves, and tidal currents. The nearshore wave breaking induces the initiation of sediment movement, and the associated alongshore current transports a large volume of sediments that tend to either accrete toward or erode from the beach face and seabed. Sediment transport rate in the nearshore waters during cyclones is higher than that under normal conditions. The measured changes due to Cyclone Nivar in November 2020 in the nearshore morphology along the Mahabalipuram coast are examined to understand the response of nearshore morphology to cyclonic wave-induced forcing. The beach-profile measurements across 10 transects at 100 m spacing covering about 1000 m along the coast were measured before and after the passage of Cyclone Nivar as a part of the present field study. The evolving beach profiles during Cyclone Nivar were simulated using the storm-induced beach change (SBEACH) model, which is a cross-shore profile evolution model. The changes due to berm erosion and deposition of nearshore sand bars have been compared from field measurements data and model prediction. The calibrated model was then used to simulate the beach profile response at two other locations along the cyclone-affected coastline to examine the shoreline impact. The calibrated model can be used along the coast to understand the poststorm profiles of the beach with reasonable accuracy.

ADDITIONAL INDEX WORDS: *Beach processes, cyclone, cross shore sediment transport, field instrumentation, storm surge, modelling.*

INTRODUCTION

Environmental forces caused by wind, waves, currents, and water-level variations determine the spatial and temporal changes in sediment transport at nearshore and in the wave-breaker zone. Among them, the stochastic variation of waves (*i.e.* height, period, direction) plays a dominant role on shoreline interaction and, in turn, the beach morphology. Waves breaking near the coast initiate the sediment to get in suspension mode in the water column, and the currents generated by wind, waves, and tides transport sediments along and across the coast. The accelerated increase in the cyclonic wave activities and the rise of water level because of storm surge add further layers of complexity to the stability of nearshore morphodynamics. Cyclones along the east coast of India are associated with high wave heights and surges in water levels, enhancing the movement of sediments from the shore front to the offshore region. The steep waves associated with cyclones erode the berms and dunes, carrying large volumes of sand toward offshore, often causing severe damages to coastal habitats.

Beaches exposed to high-energy cyclonic waves exhibit rapid and significant adjustments at shorter time scale (Leaman *et al.*, 2021; Schwarzer *et al.*, 2003; Splinter *et al.*, 2017). The past studies on nearshore morphological variation segregate the time scales of change as long term (several decades to hundreds of years), medium term (several years to decades, called interannual variability), seasonal variability (repeating on an annual cycle called intra-annual variability), and short-term extreme events. There has been an increasing interest in understanding the short-term morphodynamics and the response of beaches to single storm and storm sequences (Harley *et al.*, 2017; Masselink and van Heteren, 2014). Studying such cyclonic events and their effects on beach changes is also crucial from a socioeconomic context of the habitations near such regions.

The beach-profile classification, depending on the incident wave climate, can be used to distinguish the resulting beach profiles due to energetic storm waves and normally observed waves during the fair-weather period. Hayes and Boothroyd (1969) and King (1972) state that beach slope steepens with larger sediment size and wave energy. The studies that use field observations involving the effect on sandy-beach profiles because of storms are few because it is challenging to set up a detailed measurement campaign in anticipation of a storm event in a particular region. Hence, a detailed field-survey program must be planned well ahead of the approaching cyclone to understand the changes due to higher wave activity associated with cyclones.

The importance of the studies on beach-profile changes is directly relevant to the understanding of beach and dune response to storms, beach nourishment problems, shoreline response to

DOI: 10.2112/JCOASTRES-D-23A-00016.1 received 29 November 2023; accepted in revision 17 December 2023; corrected proofs received 26 February 2024; published pre-print online 19 March 2024.
*Corresponding author: guruprasath.jayadev@gmail.com

sea-level rise, seasonal changes of shoreline positions due to onshore-offshore transport, overwash effects, and similar phenomena.

The present study examines the changes in the nearshore morphology along the coast due to the effect of cyclones in the vicinity. A comprehensive measurements of beach profiles and nearshore bathymetry along the Mahabalipuram coast were performed during Cyclone Nivar in the Bay of Bengal to study the cyclone's impact on nearshore morphology. The effects of Cyclone Nivar on the beach profiles along the coastal stretch have been simulated using the storm-induced beach change (SBEACH) model, and the model parameters were tuned by comparing the predicted beach profiles with the measured profiles. The calibrated beach model has then been executed at two other locations in Koonimedu (cyclone landfall point) and Thalanguda (south of the cyclone landfall point).

Study Area

The detailed field measurements were undertaken along the northern coastal segment of Tamil Nadu around the landfall point of Cyclone Nivar (12°05′49″ N, 79°54′20″ E).

The present measurements focused on three locations.

(1) Mahabalipuram coast (12°36′58″ N, 80°11′56″ E), which is about 65 km north of the cyclone landfall point;
(2) Koonimedu coast in the Villupuram District (12°04′48″ N, 79°53′42″ E), which is near the landfall point of Cyclone Nivar; and
(3) Thalanguda coast near Cuddalore (11°45′50″ N, 79° 47′30″ E), which is about 38 km south of the cyclone landfall point.

The coastal segment of Mahabalipuram is located about 55 km south of Chennai, the state capital of Tamil Nadu. It is known for its architectural marvels and is recognized as a world heritage monument site by the United Nations Educational, Scientific, and Cultural Organization. The coastal stretch facing the Bay of Bengal is nearly straight and oriented N 10′ E. The coastal stretch is about 1000 m long of sandy beach marked by the 200-m-long curved seawall built to protect the world-famous Mahabalipuram shore temple. The low-level sand dunes on the back-shore parts of the beach are observed. Along this coast, the seasonal average highest significant wave height (H_s) is about 1.5 m during the NE monsoon period (October to December), and the annual average H_s is about 1.0 m. The tide is semidiurnal, with the spring tidal range of 1.1 m and neap tide range of 0.6 m. It features a typical monsoon climate highlighted by the SW and NE monsoon regimes. The study area and the transect locations along the Mahabalipuram coast for beach profile measurements are presented in Figures 1 and 2. The nearshore slopes along southern profiles 6–10 were observed to be steeper than those along northern profiles 1–5; this occurs because of the predominant northerly drift along the east coast of India, which induces sediment accretion on the south of the protruding seawall and subsequent erosion on the northern stretch. The effective sediment grain size (D_{50}) in Mahabalipuram coast is 0.2 mm to 0.4 mm. The coarser grain size is found on the southern side along profiles 6–10, whereas the finer grain size has been found on the northern side along profiles 1–5.

The other two selected coastal locations for the present study, *i.e.* Koonimedu and Thalanguda, are coastal villages in the state of Tamil Nadu. These coastal stretches are frequently exposed to natural hazards such as cyclones. The backshore of beaches in this area is relatively low level and flat, whereas the waterfront is steeper. Severe cyclones that cross the coast near these regions often cause adverse effects on the assets and natural habitats of the region. The beach sediment grain size varied from 0.3 mm to 0.5 mm.

The pre- and poststorm beach profiles available at Koonimedu and Thazanguda coasts were used in the present study to understand the model performance in predicting the beach profile response.

Cyclone Events in East Coast of India

In the present study, the coastal stretch bordering the Bay of Bengal—one of cyclogenesis areas of the world's oceans—is frequently affected by cyclonic storms during the NE monsoon months. The tracks of cyclones that had crossed the SE coast of India within 100 km on either side of the study region (from 1923 to 2022) have been analyzed, and the details of their occurrence in different months are presented in Table 1. Most of the cyclones (35 out of 43) occurred between October and December (*i.e.* during the NE monsoon period).

Cyclone Nivar

For the present study, Cyclone Nivar was considered. As per the Indian Meteorological Department cyclone bulletin reports, a low-pressure area was formed over the equatorial Indian Ocean and adjoining central parts of the south Bay of Bengal on 21 November 2020. It remained as a well-marked, low-pressure area over the SW and adjoining SE Bay of Bengal on 22 November 2020. Moving W-NW, it intensified into a deep depression on 23 November and further into the cyclonic storm, Nivar, in the early morning of 24 November. It further moved NW, turning into a very severe cyclonic storm by 25 November. Moving further NW, it crossed the coast between Pondicherry and Koonimedu (12°05′49″ N, 79°54′20″ E) from 1800–2100 (GMT) as a very severe cyclonic storm with an estimated wind speed of 120 km/h gusting to 135 km/h making its landfall. Figure 3 depicts the track of Cyclone Nivar along with the time stamp.

METHODS

An extensive field survey on beach profiles and nearshore bathymetry in the study area along the Mahabalipuram coast was taken up from 15 November 2020–9 December 2020 in two phases. The first phase was before the landfall of Nivar from 15–22 November, whereas the second phase occurred after the landfall. The survey was suspended three days before the landfall, responding to the warning issued on the intensification of the cyclone and its estimated landfall by. The cyclone landfall caused considerable disruption in the normal routines of the coastal habitats near the study area. Hence, few days were allowed for the return of normalcy in this area prior to restarting the observation campaign. The

Figure 1. The cyclone-affected coastal stretch is the study area. Detailed field measurements have been performed at Mahabalipuram (location 1); Koonimedu (location 2) is the landfall point for the cyclone; and Thazanguda (location 3) lies south of the cyclone track.

second half of the study was resumed from 2–9 December to understand the impact of the cyclone on the coast.

Measurements on nearshore currents, wave parameters, and seabed/beach sediment grain-size analysis were also performed. The site-specific data on bathymetry along with the measurements on ocean parameters serve as inputs for profile change estimation. The established cross-shore profile evolution models used to predict beach-morphology behavior during a storm rely more on accurate inputs based on such field observations. The data collected during the present study would provide a unique source for understanding the effect of cyclone-induced changes in the beach profiles.

Wave height was measured using the Datawell mini directional wave rider buoy at an offshore location (12°37′01″ N,

Figure 2. The present study considers transects numbered from 1–10. A shore-protection structure at the center of the study area divides it into north and south sections. Transects 1–5 cover the northern section, whereas transects 6–10 cover the southern section of the study area.

80°12′04″ E) in a water depth of 8 m. The bathymetry survey covered 1000 m along the coast and 500 m offshore. The echo sounder was integrated with the Differential Global Positioning System. Beach profiles were measured in the shore-normal direction from the high-tide line (HTL) to the lowest low-water mark during the spring tide period, when a maximum stretch of the beach was exposed. A Real-Time Kinematic GPS was used for the beach-profile survey. Sediment data were collected and analyzed to determine the grain size of the beach sand. A wave sled was used across the surf zone to measure the bed profiles. The wave sled was fabricated using stainless steel noncorrosive pipes with the graduated ranging staff fixed at the centre of the sled to read the values. The schematic diagram of the wave sled is given in Figures 4 and 5. The wave sled–launching coordinate of the shore point was recorded, and the sled was pulled into the sea by a boat. As the wave sled moves across the surf zone, its orientation with respect to the north is recorded, and, simultaneously, the distance of the wave sled from the shore is noted from the markings along the rope connecting the sled and the shore launching point. The water depth at the sled location was read from the markings on the staff.

Table 1. *The number of cyclones near the study area (1923 to 2022) for the past 100 years has been tabulated month-wise after analyzing the data from the Indian Meteorological Department.*

Month	Number of Cyclones
January	1
February	1
March	1
April	1
May	4
June	—
July	—
August	—
September	—
October	12
November	19
December	4
Total	43

To simulate the beach-profile evolution during a storm, the specification of the water-level variation due to local tide and the storm surge are key. In the absence of a safe location to deploy the tide

Figure 3. The observed track of the very severe cyclonic storm Cyclone Nivar over the Bay of Bengal from 22–26 Nov 2020, along with the corresponding time stamps, is depicted. The presentation illustrates the cyclone's intensification, progressing from a depression to a very severe cyclonic storm in time and space.

recorder in the coastal area, the predicted tides were used in the present study as inputs for water levels in the cross-shore profile model. In many simulations in adjacent areas, the predicted tide levels proved to be a good alternative to measured tide levels.

Water-level variation (surge histories) along the coast induced by Cyclone Nivar was simulated using the MIKE 21 flow model to understand the water-level variation in the study area due to Cyclone Nivar. This was completed by solving the shallow-water equations for given boundary conditions to compute nonsteady flow fields in response to the wind field and tidal elevation along the open-sea boundary. For model setup, three nested grids are used for the storm-surge simulation over the Bay of Bengal region. The coarser grid domain (8°34′34″ N to 23°29′07″ N, 78° 54′46″ E to 98°35′19″ E) is setup with a grid spacing of 1215 m × 1215 m, the intermediate grid system (11°49′41″ N to 12°22′22″ N, 79°45′15″ E to 80°18′13″ E) with a spacing of 405 m × 405 m, and a spacing of 135 m × 135 m is used in the finer grid domain (12°05′59″ N to 12°11′27″ N, 79°50′41″ E to 80°01′42″ E). To estimate the storm-surge height due to Cyclone Nivar at the study area, the model domain has been prepared with a nested grid arrangement (Figure 7). Murty, Flather, and Henry (1986) and Bhaskaran, Rao, and Murty (2020) have conducted

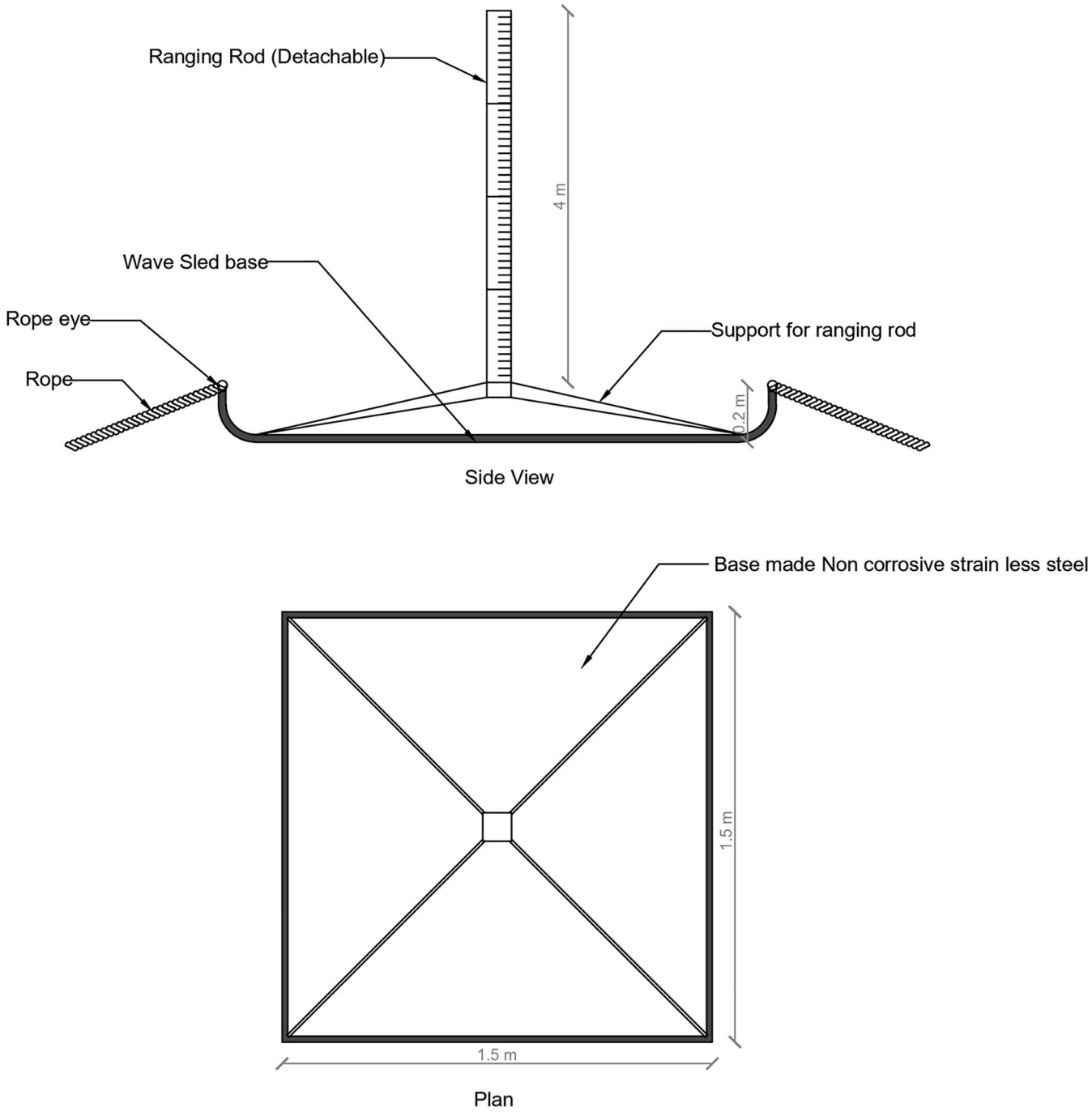

Figure 4. The diagram depicts the wave sled and its principal dimensions. The design emphasizes cost-effectiveness, making its fabrication in an academic workshop feasible. This sled is for conducting measurements in the wave-breaking zone.

similar storm-surge analyses for cyclones occurring in the Bay of Bengal. For the generation of the open-boundary condition, the Global Ocean tide database (Danish Hydraulic Institute, 2017) is used. To estimate the storm surge close to the study area due to Cyclone Nivar, the pressure and wind fields of Cyclone Nivar have been prepared as surface-forcing parameters in the model. The track of Cyclone Nivar in the Bay of Bengal and other input parameters pertaining to

Figure 5. Assembling of the wave sled at the shore is shown, as taken during the field observations.

wind field—as mentioned in the weather bulletin—were used in the simulation model.

The storm-surge height has been extracted at 12°05′46″ N and 79°54′26″ E, with a water depth of 4 m. The variation of water level has been extracted as time series, and the maximum surge due to Cyclone Nivar was estimated at the time of landfall. The maximum simulated surge during the cyclone along the Mahabalipuram coast (near the study area) was of the order of 1.5 m, and the visual reconnaissance survey from the salient marks that postcyclone landfall had been used for validation.

To simulate the beach-profile evolution during a storm, the specification of the water-level variation is important, and it is obtained from the model by introducing the predicted tide for the region over the surge response to the cyclone simulated in the flow model. The variation of predicted tide and the simulated surge history off Mahabalipuram coast during Cyclone Nivar are shown in Figure 6. The model domain for the storm-surge simulation is shown in Figure 7, and the simulated flow field at the time of landfall of Cyclone Nivar is shown in Figure 8. The movement of the cyclone along its track is such that the time of occurrence of the maximum surge during this cyclone coincides with the neap tide, which leads to comparatively lower maximum-water level.

Beach-Profile Evolution Model

Field measurements during intense, episodic events are difficult to perform, and the recourse to numerical modeling is often used to assess the short-term changes because of the effect of cyclones on beach morphology. Available models have been classified by Murray (2003) and Amoudry and Souza (2011), who report that the cross-shore, process-based modeling approach could be used over other, currently used models to study the impact of short-duration storms on beach profiles. These models rely on empiricism at specific scales. They are focused on the dominant subphenomenon, which is unlike other physics-based models that attempt to solve all the processes involved.

These process-based models, often called explicit numerical reductionist models, attempt to start bottom-up by representing processes at the smallest and fastest scales feasible and then integrate those results temporally and spatially to produce results at functional scales (Coco *et al.*, 2014). These models need to be calibrated against laboratory and field data and are relatively successful in the short-term assessment of beach-profile changes.

The typical equation governing the beach-profile evolution model in the absence of sand sources and sinks is the conservation law of sediments in the cross-shore direction:

$$\delta d/\delta t = \delta q/\delta x \tag{1}$$

where, d is the water depth from the undisturbed sea surface, and t is time. The cross-shore coordinate x' is directed positive shoreward; q is the time-averaged, cross-shore sediment transport rate that must be specified to solve the equation. The boundary conditions are zero transport at the run-up limit and insignificant cross-shore transport at some seaward point far from the coast.

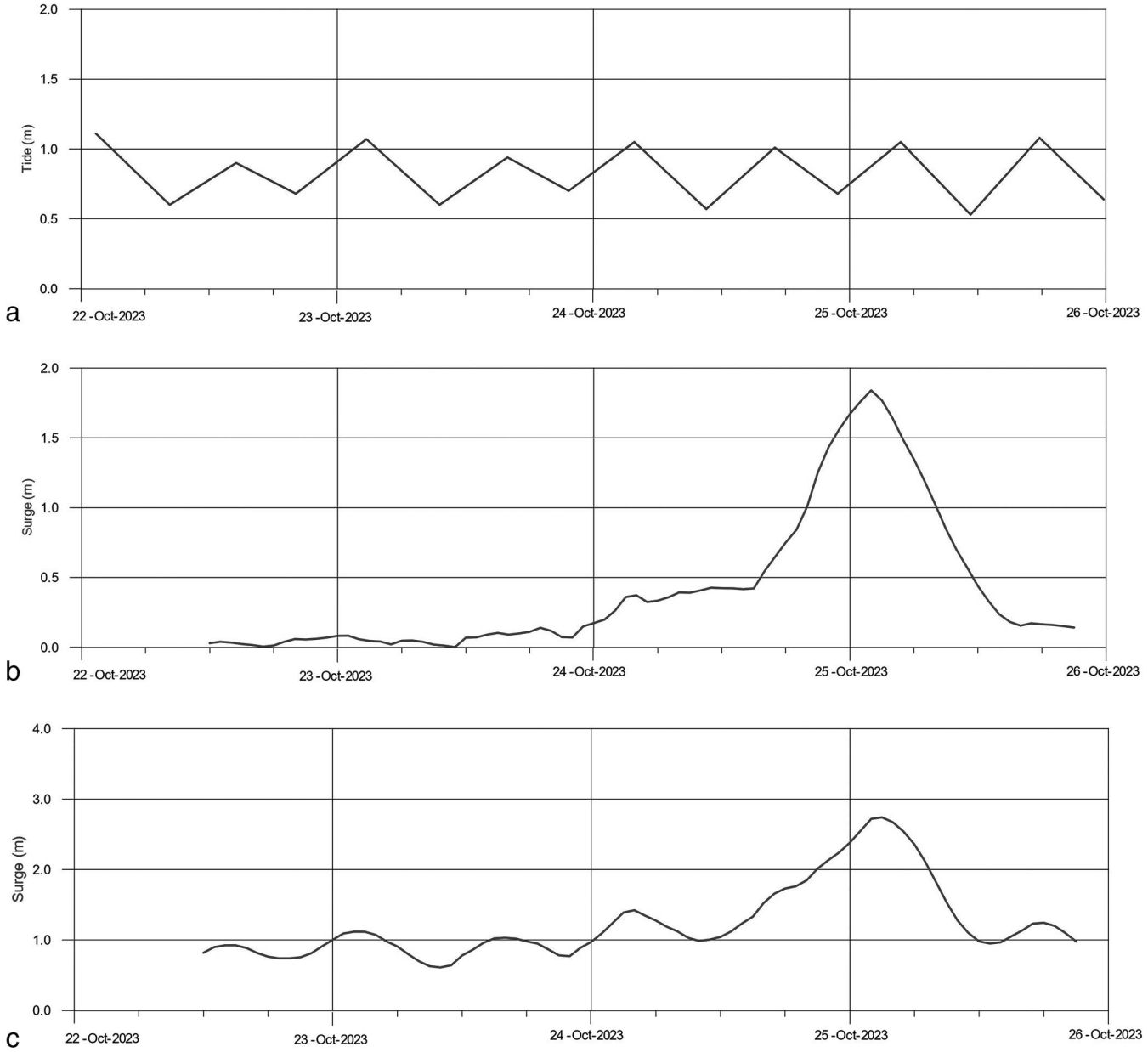

Figure 6. Display of essential information for the model simulation during the occurrence of the cyclone: (a) predicted tides, (b) simulated surge levels, and (c) combined tide and surge levels. The data presented in these components are crucial input for the model simulation.

A realistic specification of q in the models is crucial for prediction of beach-profile evolution. However, the cross-shore transport mechanism in nearshore waters is highly complex and controlled by a range of hydrodynamic processes associated with breaking waves, which may interact nonlinearly and gets influenced by the antecedent beach morphology. As the existing understanding of this cross-shore sediment transport process is only qualitative, an empirical approach is followed for the estimation of transport rate in cross-shore evolution models. In the model that estimates the cross-shore transport rate, the transformed wave field in the surf zone is first determined using the breaker-decay model of Dally, Dean, and Dalrymple (1984), and then the transport rate is estimated using the energy-dissipation model of Kriebel and Dean (1985). The direction of sediment transport in this region is determined using Larson and Kraus (1989) criterion.

To quantify the transport rate, Larson and Kraus (1989) divided the beach profile into four transport zones according to the wave characteristics across the profile (Figure 9).

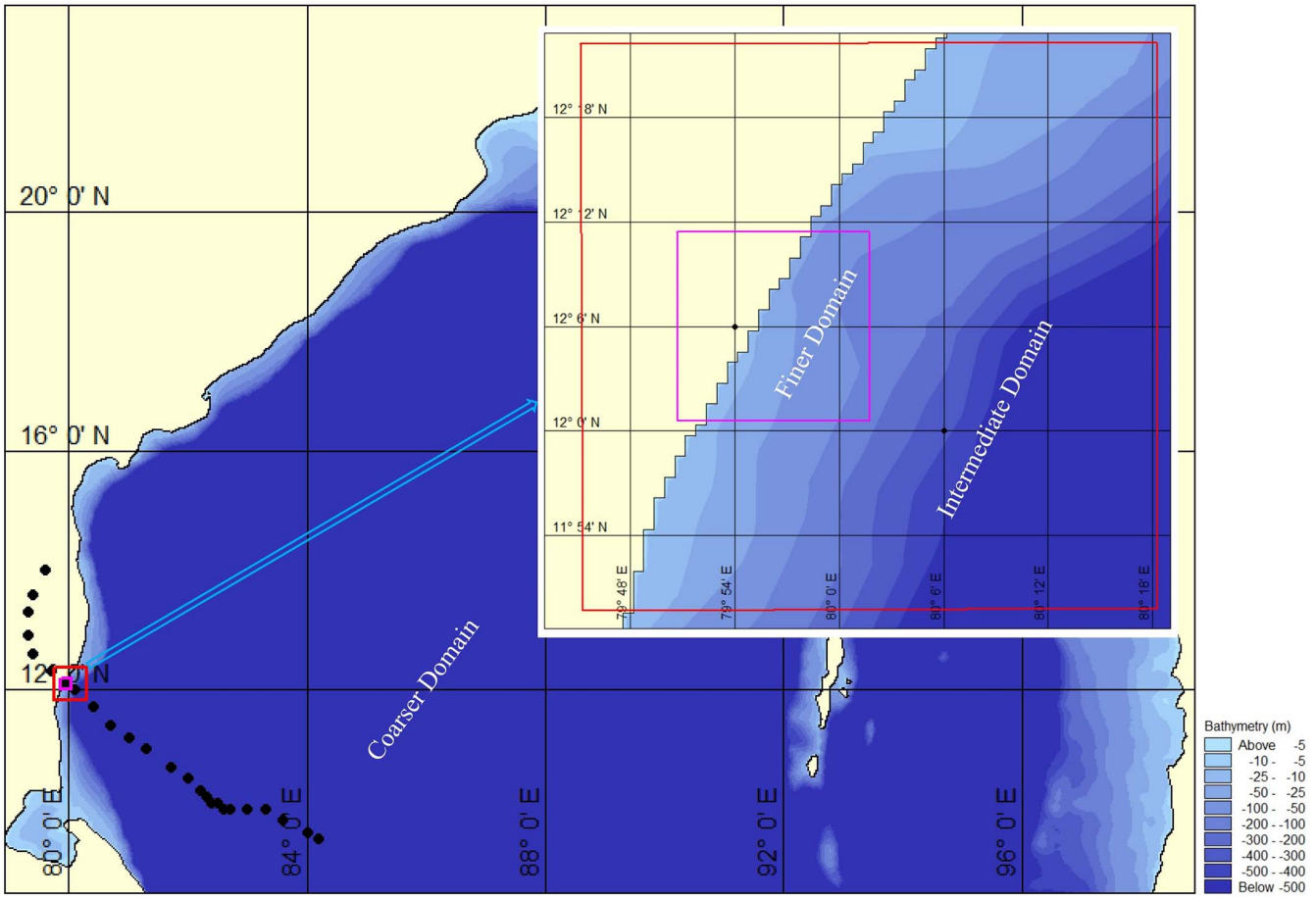

Figure 7. Three nested grids are employed for the storm-surge simulation over the Bay of Bengal region. The coarser grid domain (8°34′34″ N to 23°29′07″ N, 78°54′46″ E to 98°35′19″ E) is configured with a grid spacing of 1215 m × 1215 m. The intermediate grid system (11°49′41″ N to 12°22′22″ N, 79°45′15″ E to 80°18′13″ E) uses a spacing of 405 m × 405 m. The finer grid domain (12°05′59″ N to 12°11′27″ N, 79°50′41″ E to 80°01′42″ E) employs a spacing of 135 m × 135 m. This hierarchical grid structure enables a detailed and accurate simulation of storm-surge dynamics in the specified geographical area.

Cross-Shore, Sediment-Transport Zones and Rates

The three defined zones for the estimation of cross-shore sediment transport rate are defined here.

Zone 1

Prebreaking zone from the seaward depth of significant sand transport to the break point:

$$q(x) = q_b \ \exp\{-\in_1 (x - x_b)\} \tag{2}$$

Zone 2

Breaker-transition zone from the break point to the plunge point:

$$q(x) = q_p \ \exp\{-\in_2 (x - x_p)\} \tag{3}$$

where, subscripts b and p are quantities evaluated at the break point and plunge point, respectively. Empirically estimated, spatial-decay coefficients $\in_1$ and $\in_2$ in the transport rate of Equations (2) and (3) are given by:

$$\in_1 = 0.4 \ (D_{50}/H_b)^{0.47} \tag{4}$$

$$\in_2 = 0.2 \ \in_1 \tag{5}$$

Zone 3

Fully broken wave zone from the plunge point to the point of wave reformation or up to the offshore end of the swash zone.

In Zone 3, following Kriebel and Dean (1985), the cross-shore transport rate is assumed to be proportional to the excess energy dissipation per unit volume over an equilibrium value of energy dissipation (E_{eq}), which is defined by the amount of energy dissipation per unit volume that a beach with a specific grain size could withstand without generating significant sediment transport.

Thus, the transport rate is defined as:

$$q = K \ (E - E_{eq}) \tag{6}$$

where, E is the wave-energy dissipation per unit volume of water (N m/m^3 s), which is given in terms of the spatial

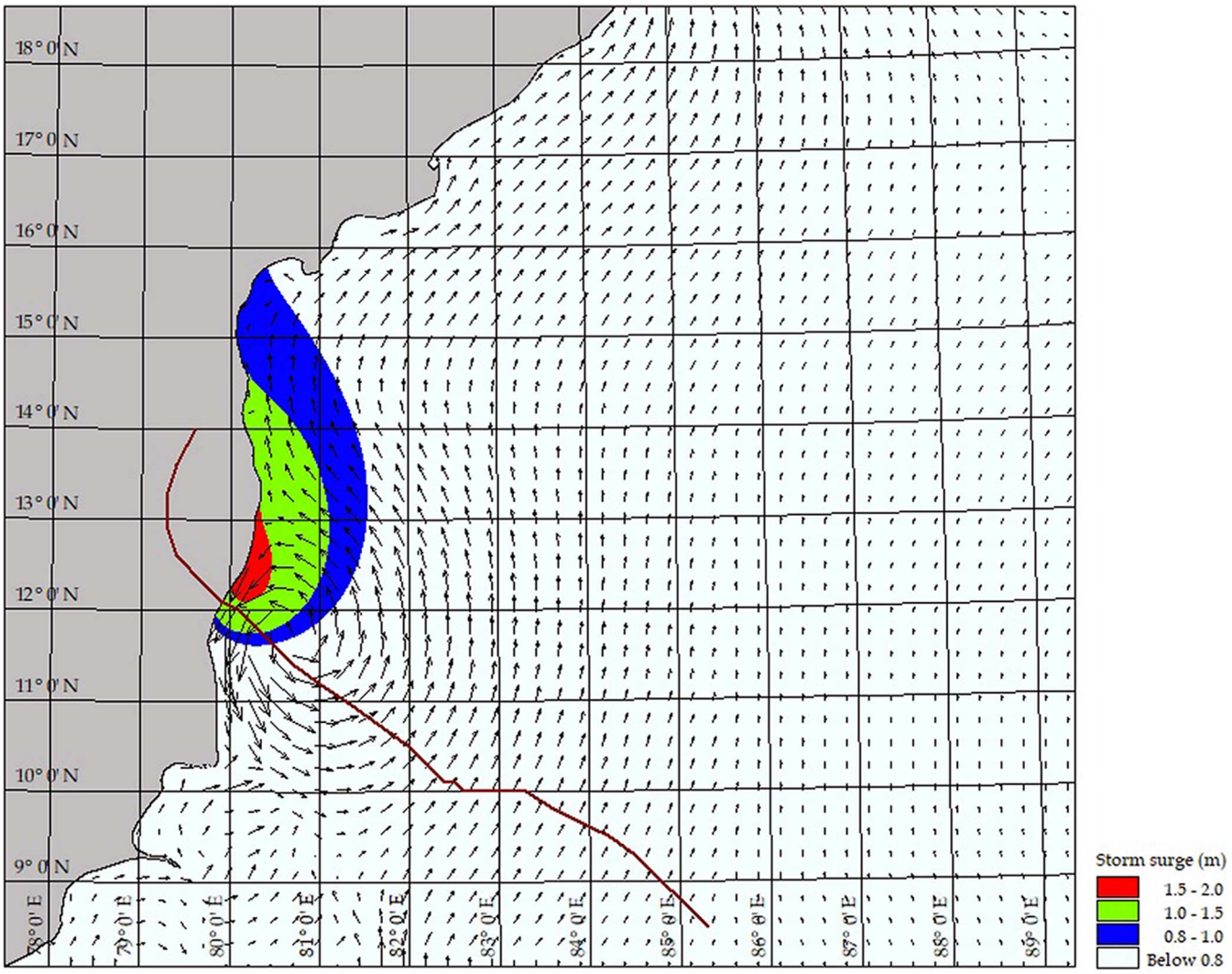

Figure 8. Storm-surge model output. Colors indicate storm-surge height: Red is 1.5–2.0 m; green is 1.0–1.5 m; blue is 0.8–1.0 m, and rest of the region is below 0.8 m.

gradient of the wave-energy flux F, and K is the transport-rate coefficient (m^4/N).

Zone 4

Swash zone from the shoreward boundary of the surf zone to the limit of the run up. The transport rate in the swash zone is assumed to decrease linearly from the end of the surf zone (Zone 3) to the run-up limit as given by:

$$q = q_z \ \{(x - x_r)/(x_z - \ x_r)\} \tag{7}$$

where, the subscripts z and r are quantities evaluated at the end of the surf zone and run-up limit, respectively.

Cross-Shore, Sediment-Transport Direction

Based on the importance of the wave-steepness parameter (H_o/L_o) and the fall-velocity parameter (H_o/wT) in the sediment-transport mechanism, the criterion to decide the transport direction (Larson and Kraus, 1989) is defined as follows.

If $(H_o/L_o) < M\ (H_o/wT)^3$, then the offshore sediment transport dominates with bar formation. If $(H_o/L_o) > M\ (H_o/wT)^3$, then the onshore transport dominates, which leads to berm formation. M is given as 0.0007, H_o is the incident wave height, L_o is the deep-water wavelength, w is the sediment fall velocity, and T is the wave period. Then, the sediment volume conservation Equation (1) can be numerically solved.

SBEACH Model

The storm-induced beach change (SBEACH) model is a semi-empirical numerical model developed by the U.S. Army Corps of Engineers for predicting the short-term, beach-profile responses to storms. This model calculates beach-profile changes that emphasize beach and dune erosion and formation and movement of the offshore sandbar. The model was initially formulated using

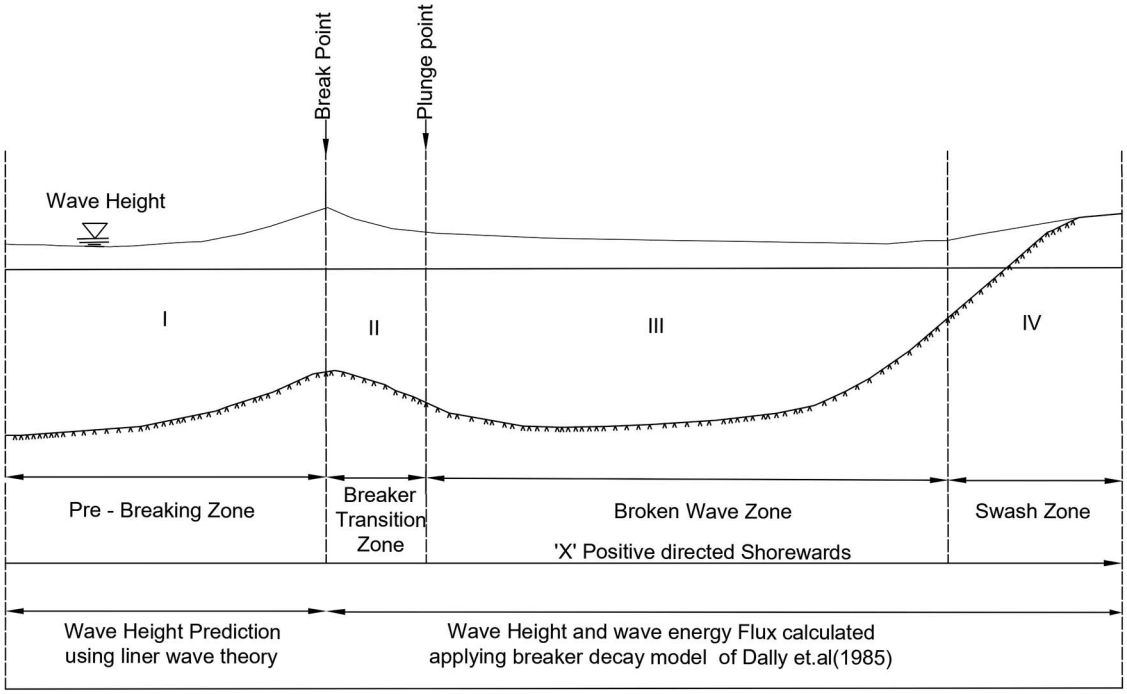

Figure 9. Classification of different cross-shore, sediment-transport zones and the theory that is applied in each zone for the numerical model, as adapted from Larson and Kraus (1989).

data from prototype-scale laboratory experiments, tuned to comply with field measurements and subjected to sensitivity testing (Larson and Kraus, 1989). To apply this model to a specific cyclonic event, it is essential to calibrate the model in the study area under similar cyclonic conditions with measurements of pre- and poststorm beach profiles. The data collected during Cyclone Nivar for this purpose are presented in the "Results" section. The theoretical basis of the SBEACH model has been described previously. The basic assumptions used in the model are as follows: The coastal region is relatively straight with parallel depth contours; wave breaking in the surf zone is responsible for beach-profile changes; small amplitude wave theory is applicable to estimate wave-height distribution up to the point of breaking; and the breaker decay model of Dally, Dean, and Dalrymple (1984) is applicable to estimate the wave-height distribution in the surf zone, and the cross-shore transport rate in different zones is calculated using different semi-empirical relationships that are valid in the zones presented in the "Cross-Shore, Sediment-Transport Zones and Rate" section.

RESULTS

The sea state was relatively calm when the field study had started on 15 November 2020. As Cyclone Nivar moved close to the East Coast of India, the roughness of the sea state gradually increased. Both the measured and the transformed wave parameters, *viz*. significant wave height (H_s), the wave propagation direction (θ), and the wave period (T), are shown in Figure 10a–c. The archived data shown are derived from the offshore wave data (H_s, θ, T) obtained from wave-rider buoy data from the Indian National Centre for Ocean Information Services (Sirisha *et al*., 2022) and transformed to a water depth of about 8 m around the boundary of the study area. The data also show that the average significant wave height varies between 0.4–1.2 m and that the mean wave period varies between 6–7 s. The wave directions remain between 45° and 150°. The wave parameters during NE monsoon months available from archived data for this region compare well with the measured parameters.

Evolution of Beach Morphology

Regions of erosion and deposition off the Mahabalipuram coast due to Cyclone Nivar, estimated from pre- and postcyclone bathymetry surveys, are shown in Figure 11.

Sediments eroded from the shore face are deposited as sand bars at 100 m to 200 m from the shoreline in a water depth of 3 m to 4 m. Existence of multiple bars that would lead to repeated wave breaking and re-shoaling are not observed. It may be noticed that the sediment volume deposited east of the seawall and immediately south of this area is significantly higher than that on the northern side of the shore temple. It implies that the net transport of sediment during this cyclone is toward north and that the central seawall around the temple acts as a barrier to the northbound transport. The quantum of erosion in the backshore of beaches, as measured by the difference in elevations between surveys, is estimated as 1.4 million m^3, and the quantum of deposition in the nearshore region is 0.9 million m^3. The deposition was dominantly observed up to a water depth of 4 m, beyond which only scattered deposition was observed.

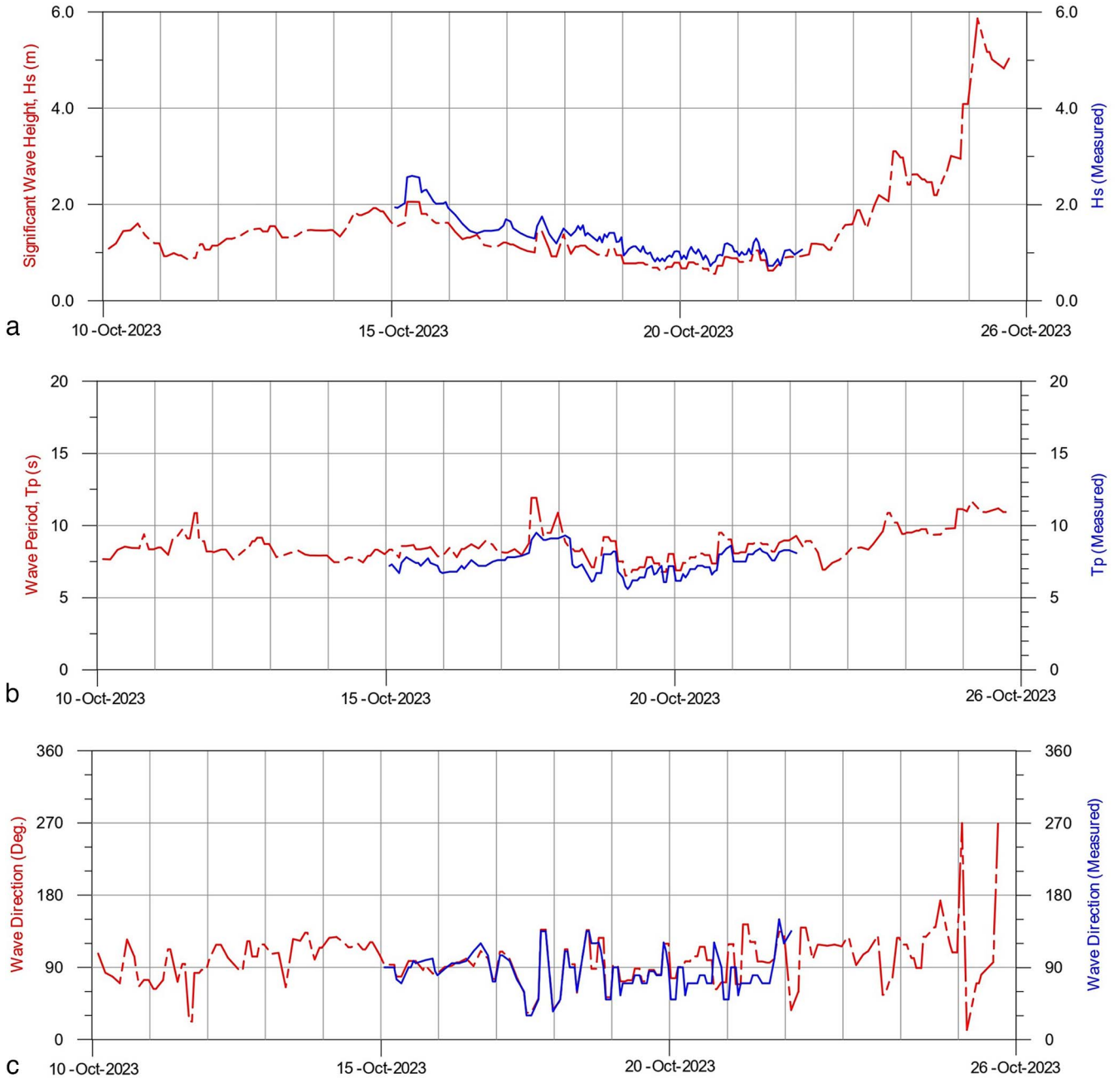

Figure 10. (a) Variation of significant wave height 10. (b) Variation of wave period 10. (c) Variation of wave direction. (Data from open source is shown in red-dashed lines, and measured data at the site are represented in blue lines.)

DISCUSSION

The beach profiles measured during pre- and postcyclone along the Mahabalipuram coast are presented in Figure 12. The offshore bars in the measured postcyclone beach profiles 2, 3 and 4 in the northern stretch are significantly higher than those along other profiles, in particular along the southern stretch. Along profiles 2 and 4, maximum bar heights were ~2 m, and along transect 3, it was ~1 m; along the remaining profiles, the bar heights were less than 0.5 m. Hence, it can be stated that the offshore sand bar due to a severe storm would form when a coastal berm exists. When the beachfront is nearly flat above the HTL, then no significant sand bar formation occurs after an extreme wave climate.

The poststorm beach profiles across all profiles were predicted using the SBEACH model. The model was first calibrated for the tuning parameters *viz*. transport-rate coefficient, its decay coefficient, effective sediment-grain size, and maximum slope prior to avalanching, which

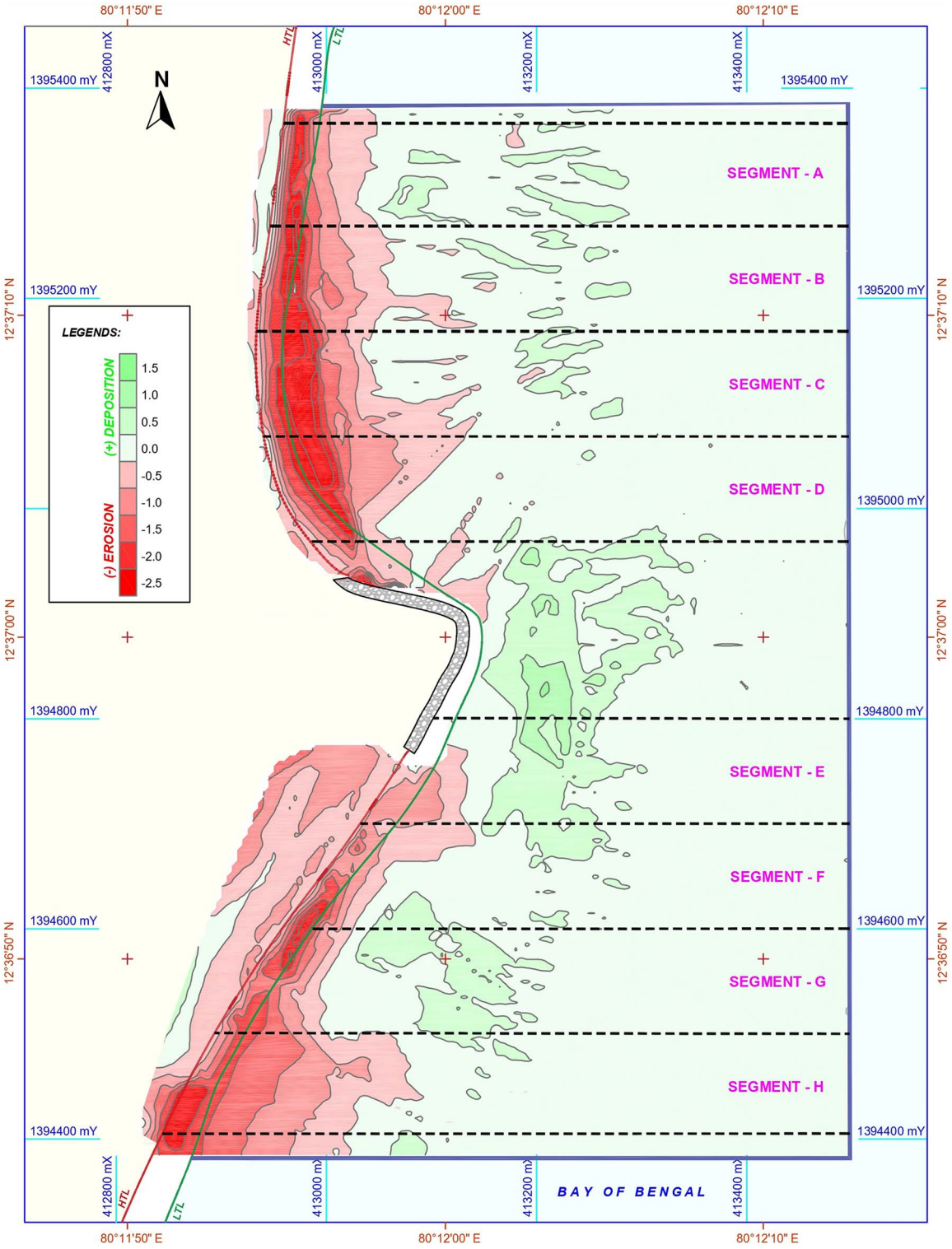

Figure 11. Illustrated regions of erosion and deposition off the Mahabalipuram coast resulting from the impact of Cyclone Nivar. These estimates are derived from pre- and postcyclone bathymetry surveys, showcasing the difference in bathymetry. The severity of erosion is represented by the red spectrum, ranging from dark red (indicating regions of maximum severity with approximately 2.5 m of erosion) to light red (indicating regions of lesser severity with around 0.5 m of erosion). Conversely, the green spectrum represents regions of sediment deposition, ranging from the green region (indicating approximately 1.5 m of deposition) to the light green region (indicating deposition between 0 and −0.5 m).

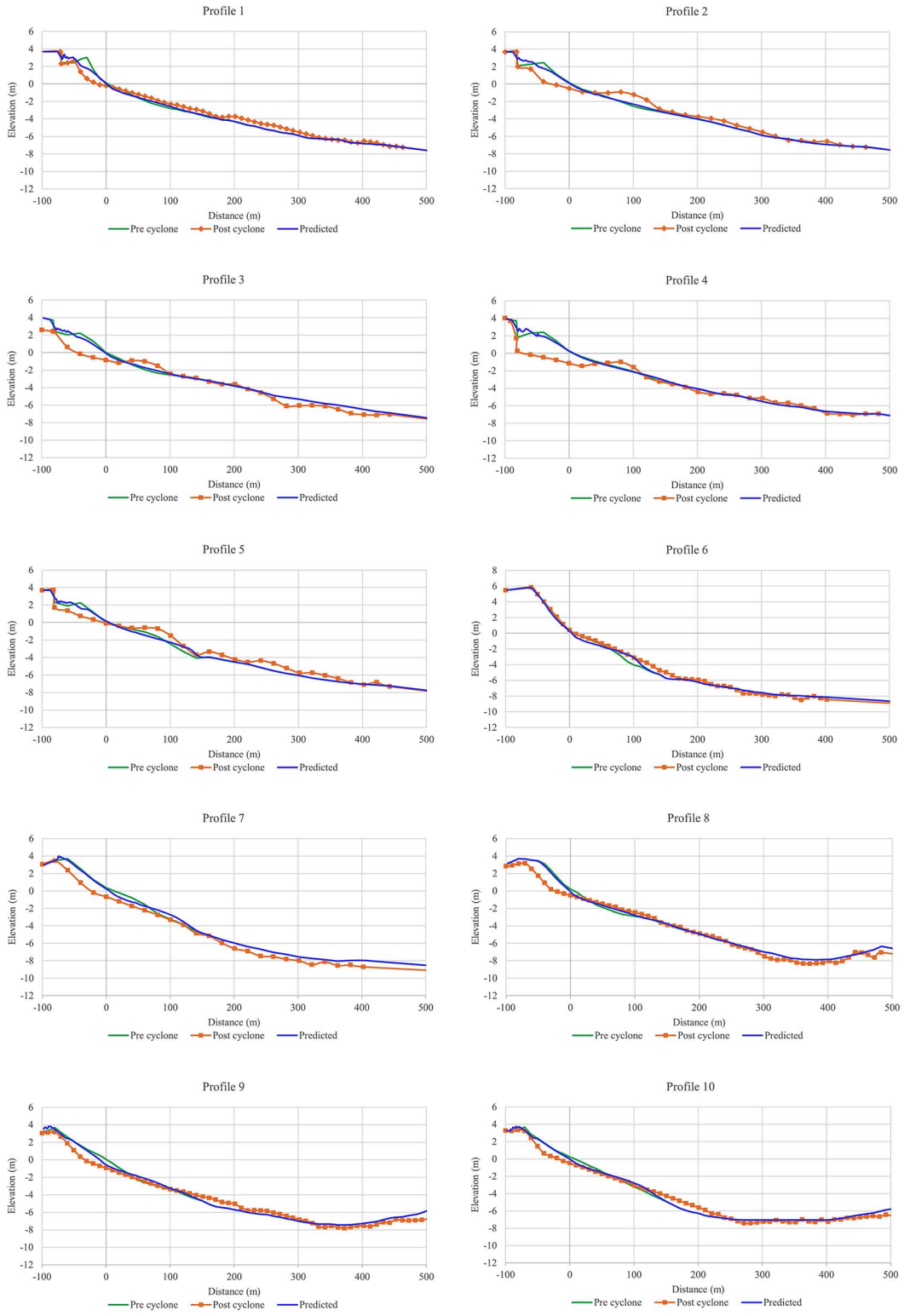

Figure 12. Profiles measured across 10 transects (1–10) both before and after the impact of Cyclone Nivar. The green line represents the profile measured before the cyclone's onset, whereas the orange line indicates the same profile measured postlandfall of the cyclone. The blue line represents the predicted profile, superimposed on the images to facilitate comparison between the measured and model-predicted profiles.

Table 2. *The table shows the calibration parameters for the SBEACH model. The first column displays the standard parameters that can be tuned. The second column presents the adapted tuning values used in the north side of the study region for profiles (1–5), whereas the third column presents the values for the south side of the study region for profiles (6–10).*

Parameter	Calibration Value (1–5)	Calibration Value (6–10)
Transport rate coefficient	2.0×10^{-6}	1.5×10^{-6}
Overwash transport parameter	0.005	0.003
Coefficient for slope-dependent term	0.002	0.002
Transport rate-decay coefficient	0.5	0.5
Landward surf-zone depth	1.2	0.8
Effective grain size	0.2	0.4
Maximum slope prior to avalanching	28	30
Water temperature	29	29

have been found to play a key role in the model predictions to obtain the best fit between the predicted and the measured beach profiles. The calibrated parameters for the coastal stretch are provided in Table 2.

The inputs to this model are the initial beach profiles, the time history of wave parameters, and the water-level history during a cyclonic storm. The measured pre- and postcyclone beach profiles and the predicted profiles are presented in Figure 12.

The coastal segments between consecutive beach profiles have been named from A to H, and the volume of sediments eroded from these segments and deposited into them are estimated and tabulated in Table 3. Similar estimates of sediment volumes have been made using the SBEACH predicted profiles as well.

The model predicts with a better agreement of more than 50% of the actual erosion from the coastal berm. The formation of well-defined offshore sand bars, *i.e.* a typical bar profile, is captured during postcyclone profile measurements. The overall measured sediment erosion in the region is about 1.3 million m^3, whereas the sediment deposited as sand bars is about 0.7 million m^3 (Table 3). The northern and southern coastal stretches are of a unique nature because of the central hard seawall, and the net erosion and deposition on the north and south of the seawall are estimated as 0.71 million m^3 and 0.38 million m^3 on the north and 0.59 million m^3 and 0.34 million m^3 on the south. Although the model prediction is better for the erosion rate, a large underprediction occurs in the deposition rate.

The difference between the erosion and deposition highlights the importance of understanding the movement of sediments from the coastal berm to the near-shore region and into deeper waters beyond the surf zone during cyclone events. The effect of the seawall as a barrier for sediment movement was also observed by the significant accumulation of sediment around the structure.

The calibrated model using measurements at the Mahabalipuram coast was extended to predict beach-profile evolution at two other locations, Koonimedu and Thazanguda coasts, which are on the coast affected by Cyclone Nivar. The pre- and postcyclone beach-profile measurements were also measured by Gracy, Sannasiraj, and Kumaran (2023). The calibrated model was found to predict the beach-profile changes well at the Koonimedu coast, which is close to cyclone landfall, and at the Thazanguda coast, which is south of the landfall. The results are presented in Figures 13 and 14.

CONCLUSIONS

The potential effect of cyclones on beach profiles and then prediction for future impact is studied by comparing field-measured profile changes to those predicted by models before and after Cyclone Nivar along the SE coast of India. A study of the history reveals that a significant percentage of cyclonic occurrences occur between October and December during the NE monsoon period and have affected the beaches along the east coast of southern Tamil Nadu. High

Table 3. *Measured and predicted volumes of sediment eroded and deposited between beach profiles during Cyclone Nivar are presented. The table has been further demarcated into northern and southern segments to understand the erosional and depositional values obtained from the measurement and simulated profiles.*

		Erosion (m^3)			Deposition (m^3)		
Segment	Between Profiles	Measured (m)	Predicted (p)	Ratio p/m	Measured (m)	Predicted (p)	Ratio p/m
Northern Segment							
A	1–2	12,900	6950	0.54	8910	3550	0.40
B	2–3	17,800	9850	0.55	11,270	4700	0.42
C	3–4	20,900	12,980	0.62	8460	3950	0.47
D	4–5	19,765	13,188	0.67	10,250	5000	0.49
Total (North)		71,365	42,968	0.60	38,890	17,200	0.44
Southern Segment							
E	6–7	9700	4320	0.45	4900	2320	0.47
F	7–8	18,100	11,000	0.61	11,200	6320	0.56
G	8–9	16,220	7310	0.45	9500	3350	0.35
H	9–10	14,910	8900	0.60	8600	3310	0.38
Total (South)		58,930	31,530	0.54	34,200	15,300	0.44
Total (North + South)		130,295	74,498	0.57	73,090	32,500	0.44

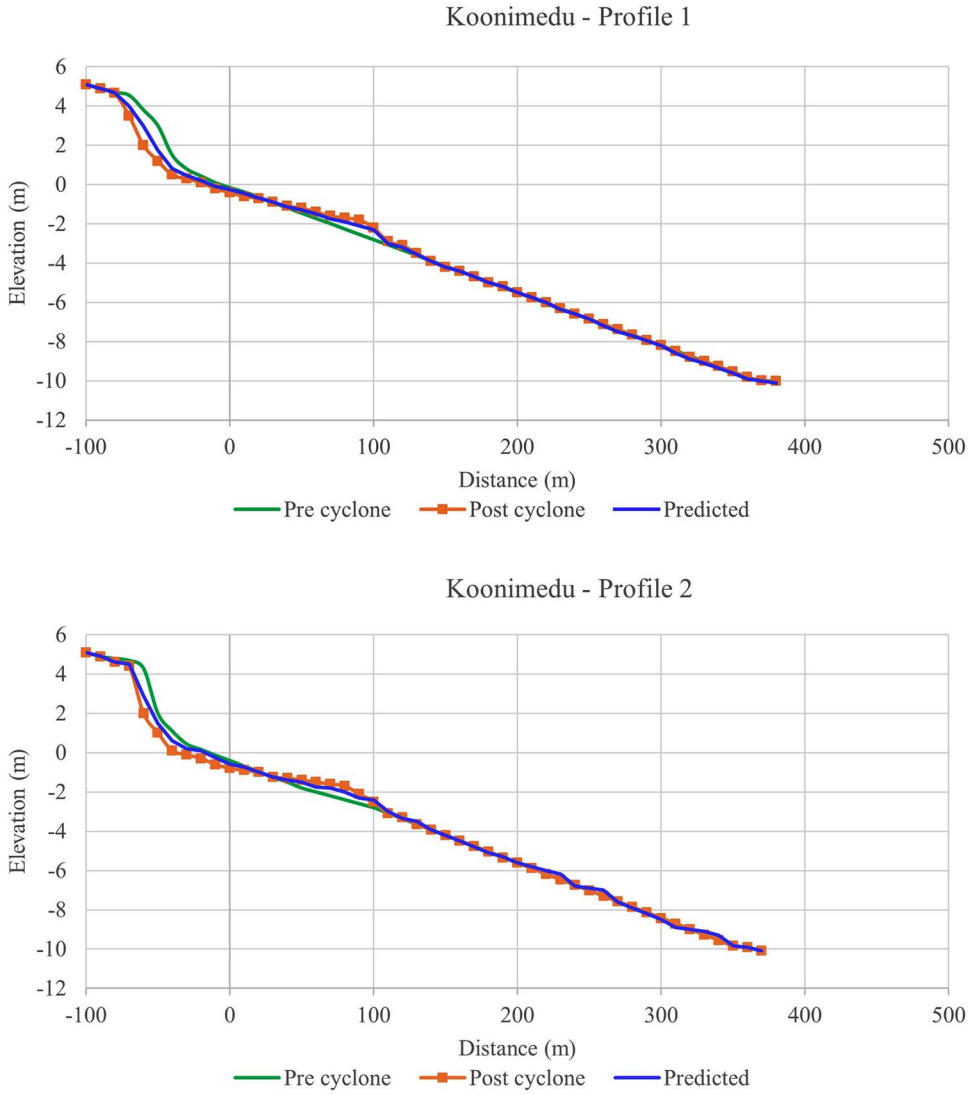

Figure 13. Measured beach profile pre- and post-Cyclone Nivar and the predicted profiles at Koonimedu. Green line indicates the initial profile precyclone, orange dotted line indicates the profile measured postcyclone, and blue line is the model predicted profile.

waves and prolonged beach flooding during Cyclone Nivar have caused severe erosion along the southern Tamil Nadu coast at many locations. Quantifying the volumes of beach eroded along the Mahabalipuram coastal stretch and the deposition in the nearshore region as sandbars is attempted. Beach surveys and anecdotal accounts by locals confirm that the beaches and dunes of Mahabalipuram have been continuously experiencing moderate erosion from the higher wave activity experienced during the cyclone periods. Lower back beach elevation and diminished dune volume in the northern part of the study region along northern transects have allowed deeper wave penetration and more significant sand removal by the cyclonic storm surge.

The study summarizes the distribution of erosional and accretional regions and shows how the sediments eroded from the shore face get deposited as offshore sand bars and a part of the sediment may even move into the deeper water zones.

The effects of Cyclone Nivar on the beach profiles along this coast were simulated along 10 profiles across the coastline using the SBEACH model. The predicted beach profiles compare well with the measured berm-bar movement across the shore after calibration. The calibrated SBEACH model was also found to accurately predict the beach-profile changes at the Koonimedu coast, which is close to Cyclone Nivar landfall, and the Thazanguda coast, which is south of the landfall.

The nearshore profile changes in the surf zone are highly dynamic and challenging to capture using conventional techniques. Studying the effects of episodic events, such as storms on beach-profile evolution, needs careful planning. Knowledge of cyclone history and of IMD cyclone warning bulletins reporting cyclonic activities in the Bay, *i.e.* updates of the current position of the cyclone, intensity, and probable cyclone track, can help in the selection of coastal measurement locations, plan

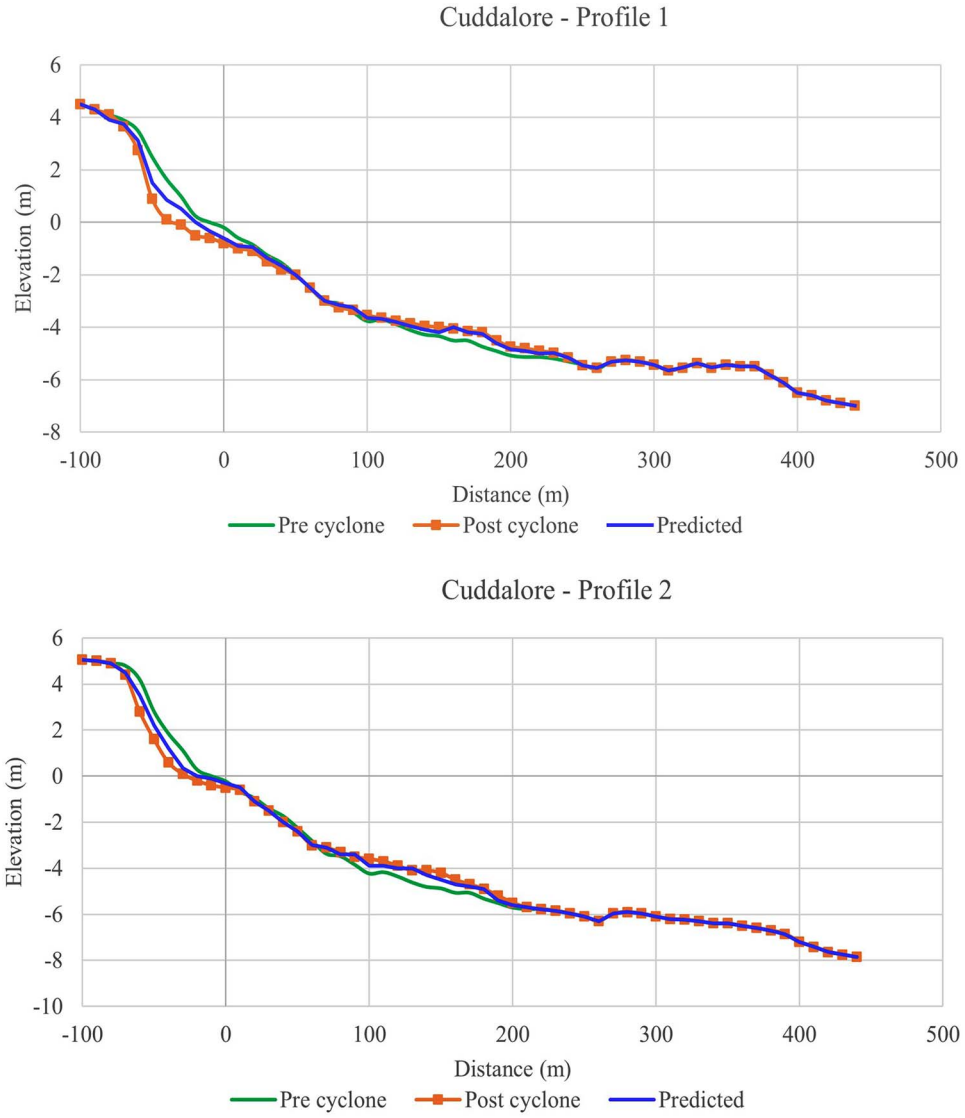

Figure 14. Measured beach profile pre- and post-Cyclone Nivar and the predicted profiles at Thalanguda. Green line indicates the initial precyclone profile, orange dotted line indicates the profile measured postcyclone, and blue line indicates the model-predicted profile.

measurement schedule, and mobilize resources in time for field measurements.

ACKNOWLEDGMENTS

This work is supported by the Department of Science and Technology, India Grant No. DST/CCP/CoE/141/2018C under SPLICE—Climate Change Program.

LITERATURE CITED

Amoudry, L.O. and Souza, A.J., 2011. Deterministic coastal morphological and sediment transport modeling: A review and discussion. *Reviews of Geophysics*, 49(2), 10–12.

Bhaskaran, P.K.; Rao, A.D., and Murty, T., 2020. Tropical cyclone–induced storm surges and wind waves in the Bay of Bengal. *In:* Srivastava P.K., Singh, S.K., Mohanty, U.C., and Murty, T. (eds.), *Techniques for Disaster Risk Management and Mitigation*. Hoboken, New Jersey: Wiley, pp. 237–294.

Coco, G.; Senechal, N.; Rejas, A.; Bryan, K.R.; Capo, S.; Parisot, J.P.; Brown, J.A., and MacMahan, J.H.M., 2014. Beach response to a sequence of extreme storms. *Geomorphology*, 204, 493–501.

Dally, W.R.; Dean, R.G., and Dalrymple, R.A., 1984. A model for breaker decay on beaches. *Coastal Engineering*, 1, 6. doi:10.9753/icce.v19.6

Danish Hydraulic Institute, 2017. *MIKE 21 Global Tide Model*. Horsholm, Denmark: Danish Hydraulic Institute. https://www.mikepoweredbydhi.com/download/product-documentation

Gracy Margret Mary, R., Sannasiraj, S. A., & Raju, D. K. 2024. Coastal morphological changes due to the Nivar cyclone on the East Coast of India. *Environmental Earth Sciences,* 83, 83.

Harley, M.D.; Turner, I.L.; Kinsela, M.A.; Middleton, J.H.; Mumford, P.J.; Splinter, K.D.; Phillips, M.S.; Simmons, J.A.; Hanslow, D.J., and Short, A.D., 2017. Extreme coastal erosion enhanced by anomalous extratropical storm wave direction. *Scientific Reports*, 7(1), 6033.

Hayes, M.O. and Boothroyd, J.C., 1969. Storms as modifying agents in the coastal environment. *In:* Larsen, F. D. and Hartshorn, J. H. (eds.), *Coastal Environments*. Amherst, Massachusetts: University of Massachusetts, pp. 290–315.

India Meteorological Department (IMD), 2020. *Very Severe Cyclonic Storm 'NIVAR' over the Bay of Bengal*. New Delhi: Cyclone Warning Division, 42p.

King, C.A.M., 1972. *Beaches and coasts*, 2nd edition. 570. United Kingdom: Edward Arnold, 570p.

King, C.A.M. and Mather, P.M., 1972. Spectral analysis applied to the study of time series from the beach environment. *Marine Geology*, 13(2), 123–142.

Kriebel, D.L. and Dean, R.G., 1985. Numerical simulation of time-dependent beach and dune erosion. *Coastal Engineering*, 9(3), 221–245.

Larson, M. and Kraus, N.C., 1989. *SBEACH: Numerical Model for Simulating Storm-Induced Beach Change*. Vicksburg, Mississippi, *Technical Report CERC-89-9, Report 1*, Empirical Foundation and Model Development, 256p.

Leaman, C.K.; Harley, M.D.; Splinter, K.D.; Thran, M.C.; Kinsela, M.A., and Turner, I.L., 2021. A storm hazard matrix combining coastal flooding and beach erosion. *Coastal Engineering*, 170, 104001.

Masselink, G. and van Heteren, S., 2014. Response of wave-dominated and mixed-energy barriers to storms. *Marine Geology*, 352, 321–347.

Murray, A.B., 2003. Contrasting the goals, strategies, and predictions associated with simplified numerical models and detailed simulations. *In:* Wilcock, P.R. and Iverson, R.M. (eds.), *Prediction in Geomorphology*, Washington, D.C: *American Geophysical Union*, pp. 151–168.

Murty, T.S.; Flather, R.A., and Henry, R.F., 1986. The storm surge problem in the Bay of Bengal. *Progress in Oceanography*, 16(4), 195–233.

Schwarzer, K.; Diesing, M.; Larson, M.; Niedermeyer, R.-O.; Schumacher, W., and Furmanczyk, K., 2003. Coastline evolution at different time scales—Examples from the Pomeranian Bight, southern Baltic Sea. *Marine Geology*, 194(1–2), 79–101.

Sirisha, P.; Remya, P.G.; Janardhanan, J., and Balakrishnon Nair, T.B., 2022. Seasonal variation of wave power potential in the coastal areas of India. *Current Science*, 122(5), 584–590.

Splinter, K.D.; Turner, I.L.; Reinhardt, M., and Ruessink, G., 2017. Rapid adjustment of shoreline behavior to changing seasonality of storms: Observations and modelling at an open-coast beach. *Earth Surface Processes and Landforms*, 42(8), 1186–1194.